HHS Public Access

Author manuscript

J Neuroimmune Pharmacol. Author manuscript; available in PMC 2022 June 01.

Published in final edited form as:

J Neuroimmune Pharmacol. 2021 June ; 16(2): 289–305. doi:10.1007/s11481-020-09914-x.

Alterations of brain signal oscillations in older individuals with HIV infection and Parkinson's disease

Eva M. Müller-Oehring[1,2], **Jui-Yang Hong**[1], **Rachel Hughes**[3], **Dongjin Kwon**[1], **Helen Brontë-Stewart**[4,5], **Kathleen L. Poston**[4,5], **Tilman Schulte**[1,3]

[1]Neuroscience Program, Center for Health Sciences, SRI International, Menlo Park, CA

[2]Department of Psychiatry & Behavioral Sciences, Stanford University, Stanford, CA

[3]Department of Psychology, Palo Alto University, Palo Alto, CA

[4]Department of Neurology & Neurological Sciences, Stanford University, Stanford, CA

[5]Department of Neurosurgery, Stanford University, Stanford, CA

Abstract

More than 30 years after the human immunodeficiency virus (HIV) epidemic, HIV patients are now aging due to the advances of antiretroviral therapy. With immunosenescence and the susceptibility of dopamine-rich basal ganglia regions to HIV-related injury, older HIV patients may show neurofunctional deficits similar to patients with Parkinson's disease (PD). We examined the amplitudes of low frequency fluctuations (ALFF) across different frequency bands of the BOLD signal in 30 older HIV-infected individuals, 33 older healthy controls, and 36 PD patients. Participants underwent resting-state fMRI, neuropsychological testing, and a clinical motor exam. HIV patients mainly showed abnormalities in cortical ALFF with reduced prefrontal amplitudes and enhanced sensorimotor and inferior temporal amplitudes. Frontal hypoactivation was overlapping for HIV and PD groups and different from controls. PD patients further exhibited reduced pallidum amplitudes compared to the other groups. In the HIV group, lower pallidum amplitudes were associated with lower $CD4^+$ nadir and $CD4^+$ T cell counts. Abnormalities in ALFF dynamics were largely associated with cognitive and motor functioning in HIV and PD groups. The disruption of neurofunctional frequency dynamics in subcortical-cortical circuits could contribute to the development of cognitive and motor dysfunction and serve as a biomarker for monitoring disease progression with immunosenescence.

Graphical Abstract

Address correspondence to: Eva M. Müller-Oehring, Ph.D., Department of Psychiatry and Behavioral Sciences, Stanford University School of Medicine, 401 Quarry Rd, Stanford, CA 94305, Phone: +1 650 859-2767, Fax: +1 650 859-2743, evamoe@stanford.edu.

Conflict of Interest Statement

The authors declare that they have no conflict of interest.

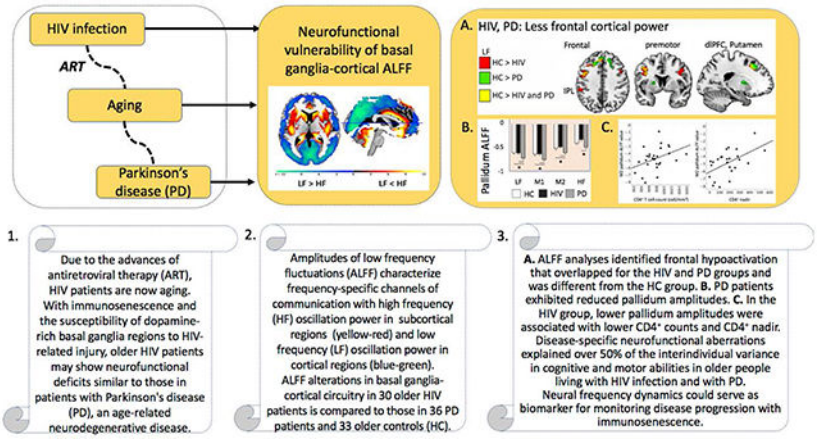

Keywords

age; amplitudes of low frequency fluctuations (ALFF); HIV infection; Parkinson's disease; resting-state fMRI

Introduction

Since the introduction of successful treatment for human immunodeficiency virus (HIV) via antiretroviral therapy (ART), individuals infected with HIV are now living longer, with life expectancies comparable to those in the general population (van Sighem et al., 2010). Yet, the development of cognitive impairments and milder forms of HIV-associated neurocognitive disorder (HAND) occur frequently despite effective treatment with ART and viral suppression in blood and CSF (Heaton et al., 2010; Chaganti et al., 2017), potentially in relation to immunosenescence and chronicity of viral infection in the central nervous (Morgan et al., 2012), which warrants a need to research the effects of chronic HIV infection and aging on neuropathology.

Subcortical systems appear to be most susceptible to HIV-related injury, with HIV viral replication resulting in significant neuronal loss in dopamine-rich brain regions such as the substantia nigra (Khanlou et al., 2009) and basal ganglia (BG; Berger and Arendt, 2000; Kumar et al., 2011; Tesic et al., 2018). Disruption of BG functioning also appears to impact other dopaminergic systems, including the frontostriatal network (Berger and Arendt, 2000; Melrose et al., 2008; Brew et al., 2009). Deregulation of dopaminergic BG-cortical systems may underpin motor disturbances and cognitive deficits (Brew et al., 2009; Kumar et al., 2011). Indeed, the neuropathological changes in dopaminergic systems and the BG in HIV are similar to the functional alteration in BG circuits in Parkinson's disease (PD) (Esposito et al., 2013; Wang et al., 2018) that occur subsequent to striatal dopamine depletion (Dauer and Przedborski, 2003), such as altered firing rates and pathologic oscillatory activity (Galvan et al., 2015).

Functional brain imaging can provide insight into the pathogenesis of cognitive compromise and motor disturbances in older virally-controlled HIV patients on ART. Recently, there has been an increase in the utilization of resting-state functional magnetic resonance imaging

(rs-fMRI) because of its usefulness in identifying abnormalities in the intrinsic neurofunctional architecture. rs-fMRI typically examines blood oxygenation level dependent (BOLD) signal oscillations at low frequency (LF) bandwidths between 0.01 Hz and 0.1 Hz (e.g., Fox and Raichle, 2007). However, BOLD signals oscillate systematically at different frequencies within the signal bandwidth and are organized in a resting brain (Zuo et al., 2010) such that lower LF oscillations facilitate long-distance communication across cortical regions, whereas higher oscillations occur predominantly in closely localized, subcortical areas (Baria et al., 2011). For example, Zuo et al. (2010) found higher rs-fMRI fractional amplitude of low-frequency fluctuations (ALFF) in the BG at a frequency band of 0.027-0.073 Hz than that at 0.01-0.027 Hz. To better distinguish between these frequency band oscillations across brain regions, analyses employing the ALFF (Zou et al., 2008) at different bandwidths were created, which may capture HIV-related BG and cortical neurofunctional characteristics most accurately.

Recent studies on the neuropathological changes in dopaminergic systems calculated ALFF in PD patients, in comparison to healthy subjects, and found reduced ALFF in the BG (Hu et al., 2015; Li et al., 2017; Wang et al., 2018), cortical sensorimotor regions (pre- and postcentral gyri) (Hu et al., 2015; Li et al., 2017; Wang et al., 2018), and the cerebellum (Hu et al., 2015). Since brain dysfunction involving the BG and cortical circuits may ensue and potentially progress over the course of HIV infection, recent studies have consequently started to examine the pattern of frequency band-dependent oscillations in HIV patients. To this end, Li and colleagues (2019) investigated the early course of HIV infection and found ALFF abnormalities in several brain regions including striatal, frontoparietal, and occipital regions in recently infected adults relative to seronegative controls. In a study on chronic HIV infection, Bak et al. (2018) reported decreases in bilateral frontal ALFF and increases in regional homogeneity in sensorimotor areas that were related to HIV-associated neurocognitive disorder status. These recent studies provide the first evidence that ALFF aberrations can occur early in the disease and persist with chronic HIV-infection despite ART.

While resting-state functional neuroimaging is particularly useful in identifying abnormalities in intrinsic functional architecture, it has not yet been fully utilized in HIV studies. ALFF may have the potential for detecting neurofunctional compromise in older HIV-infected individuals, and ALFF alterations in BG-motor circuitry may show similarities to those in other age-related neurodegenerative diseases, such as PD. Though ALFF alteration could serve as a biomarker for cognitive and motor dysfunction, no study has examined this methodology in older HIV patients. Consequently, the aim of this study was to analyze the effect of HIV infection on the brain's frequency oscillation power dynamics as a means for understanding the pathogenesis of functional compromise in older virally-controlled patients on ART. We hypothesized that (1) relative to older seronegative controls, older HIV-infected individuals exhibit altered ALFF values in subcortical and cortical brain regions and, in comparison with PD patients, show similarities in neurofunctional BG-cortical oscillation power dynamics. (2) ALFF alterations are neural correlates of behavior such that more signal aberrations in HIV and PD (relative to controls) in motor cortical, BG, and cerebellar regions would be related to motor functional compromise, while ALFF power

in frontal, temporal, parietal, and occipital cortical regions would be related to cognitive performance.

Materials and Methods

Subjects.

The sample included 30 individuals with HIV infection (11 women), 36 individuals who met criteria for mild to moderate idiopathic PD (14 women) (Litvan et al., 2012), and 33 healthy controls (HC) (18 women). Healthy subjects were recruited from advertisements or web-postings, HIV participants through referrals from community physicians and HIV treatment centers, and PD participants through San Francisco Bay Area PD events, community treatment centers, support groups including the Michael J. Fox trial finder and Stanford Department of Neurology and Neurological Sciences (Drs. Bronte-Stewart and Poston labs). The recruitment and study protocols were approved by the Institutional Review Boards of Stanford University School of Medicine and SRI International. All subjects provided written informed consent and underwent a clinical examination, neuropsychological testing, and neuroimaging.

At the time of testing, all participants were at least 45 years old. All participants were screened for schizophrenia or bipolar disorder, neurological disease other than PD, medical conditions potentially affecting the central nervous system other than HIV, or MRI contraindications. Screening was conducted by physicians, clinical research psychologists or research nurses. HC participants screened negative for psychiatric conditions and abnormal cognitive functioning determined through Structured Clinical Interview for DSM-IV (First et al., 1998), and neuropsychological assessment. All participants screened negative for dementia using the Dementia Rating Scale (DRS-2; Jurica et al., 2004), and groups did not differ across DRS-2 scores or verbal IQ estimates using the Wechsler Test of Adult Reading (WTAR-SS; Wechsler, 2001). The PD group was on average older than the HIV and HC groups (Table 1). All groups had average education levels beyond high school, although the HIV group had less years of education than the HC and PD groups. Both patient groups had lower global cognition scores than the HC group after controlling for age and education (Table 1).

Clinical assessment.

The diagnosis criteria for HIV patients included seropositive on HIV test, nadir $CD4^+$ T cell counts >200 cell/mm^3, and at least 2 months of continuous antiretroviral therapy. In the HIV group, the mean $CD4^+$ T cell count at time of the study was 763±299 cell/mm^3 (range between 221 and 1576 cell/mm^3; normal range: 490-1740 cell/mm^3). $CD4^+$ nadir values represent the lowest T cell counts in an individual's HIV disease history. The group's mean $CD4^+$ nadir was 183±139 (0-550) cell/mm^3. Out of 24 HIV participants, 16 met criteria for AIDS ($CD4^+$ nadir<200 cell/mm^3 and/or AIDS-defming event) sometime during the course of their illness. On average, HIV subjects had been diagnosed 26±8 (6-40) years ago. Individuals were on average 34±9 (18-49) years old when diagnosed with HIV.

PD patients in the study had mild to moderate Parkinson severity (Gelb et al., 1999), a diagnosis duration of at least 2 years, and symptom improvement on dopaminergic medication as measured by part III of the Movement Disorder Society -Unified Parkinson's Disease Rating Scale (MDS-UPDRS, 2003) and determined by a neurologist (Supplementary Table S1). Dopaminergic medication comprised a combination of MAO-B inhibitors, dopamine agonists (DA), and/or levodopa (1-dopa). The mean levodopa-equivalent daily dose (LEDD) was 567±283 (100-1440) mg (see Herzog et al., 2003 for LEDD calculation from treatment regimens). PD subjects had been diagnosed on average 4.7±2 (1.95-11) years ago.

Motor exam.

All participants underwent a neurological examination and clinical motor exam by a movement disorder specialist or trained assistant at the Stanford Movement Disorders Center. PD participants underwent motor testing twice, on and off dopaminergic medication. Ataxic motor signs were tested using the Scale for Assessment and Rating of Ataxia (SARA; Schmitz-Hübsch et al., 2006). Supplementary Table S1 describes the clinical motor symptoms for each group, and for PD patients on- and off-dopaminergic medication.

Neuropsychological assessment.

Neuropsychological tests examined information processing (IP) speed (Symbol Digit Modalities Test, SDMT-oral; Smith, 1973, 1982) executive control (Golden Stroop Task; Golden, 1978; Digit Span Backward; Wechsler Memory Scale-Revised [WMS-R], Wechsler, 1987), attention (digit span forward; WMS-R), visuospatial processing (Judgement of Line Orientation [JLO], Benton et al., 1983), and verbal memory (California Verbal Learning Test-II [CVLT-II], Delis et al., 2000). To diminish the impact of motor deficits on cognitive outcome measures in individuals with PD, we examined cognitive functions in PD patients on dopaminergic medication, as recommended by published guidelines (Litvan et al., 2012). Supplementary Table S2 describes the cognitive performance raw scores for each group. For additional information on correlations among clinical motor and cognitive test scores, see Supplementary Table S3.

Imaging data acquisition.

Whole brain resting-state fMRI (rs-fMRI) data was obtained by General Electric MR750 system with an 8-channel head coil while subjects kept their eyes open in the scanner. PD participants were tested on dopaminergic medication. The rs-fMRI images were acquired with a T2*-weighted 2D axial echo-planar pulse sequence (echo time [TE]=30 ms; repetition time [TR]=2000 ms; flip angle=90°; matrix=128×128; slice thickness=5 mm). For spatial registration purpose, a 3D fast spin-echo scan was obtained using the following parameters: TE=100.066 ms; TR=2500 ms; flip angle=90°; matrix=512×512; slice thickness=1.2 mm. To correct for spatial distortions in the echo-planar images, a field map was acquired with a 2D gradient-recalled echo sequence pair (TE=9 ms; TR=1000 ms, slice thickness=5 mm; flip angle=60°; matrix=64×64).

Image preprocessing.

rs-fMRI data preprocessing was performed using Statistical Parametric Mapping 12 (SPM12) software (Wellcome Department of Cognitive Neurology; http://www.fil.ion.ucl.ac.uk/spm/software/spm12/). Images were first converted from DICOM into NIFTI format followed by spatial realignment and unwarping of echo-planar images with field map images to correct for geometric distortion. All data were inspected for quality and movement artifacts based on SPM12 motion correction parameters and ArtRepair Software (http://cibsr.stanford.edu/tools/human-brain-project/artrepair-software.html). The average translational movement and rotational absolute motion of all images did not exceed 2 mm translation in x, y, z, and 2° rotation in all three directions. In addition, no more than 15% of total images within each subject exceeded the frame-to-frame movement threshold (0.3 mm/TR) based on ArtRepair Software (see also Power et al., 2015). Frame-wise displacement values were calculated for individual scans, with the mean displacement at 0.098 mm (standard deviation=0.08 mm). Groups did not differ in head motion (mean frame-wise displacement; $F(2,96)=0.97$, ns; median frame-wise displacement; $F(2,96)=0.99$, ns). For each subject, the mean unwarped functional images were coregistered with the anatomical images, then normalized to the standard Montreal Neurological Institute (MNI) space, and resampled to a voxel size of 2×2×2 mm. A Gaussian kernel of 8 mm full-width at half-maximum was applied to the normalized functional images.

Amplitude of Low Frequency Fluctuation (ALFF) calculation.

Preprocessed functional images were imported into DPABI v2.3 toolbox (Data Processing &Analysis of Brian Imaging; http://rfimri.org/dpabi) for ALFF calculation (Yan et al., 2016). A Fast Fourier Transform was used to obtain the frequency power spectrum with the time series of each voxel within the individual functional images transformed into the frequency domain. The full frequency range was then divided into four frequency bands—low frequency (LF) (0.01-0.027 Hz), middle frequency 1 (M1) (0.027-0.073 Hz), middle frequency 2 (M2) (0.073-0.17 Hz) and high frequency (HF) (0.17-0.25 Hz)—for further ALFF value calculation (Esposito et al., 2013). Standardized ALFF individual maps were applied, based on evidence showing reduced motion effects at individual level and increased test-retest reliability with Z-standardization at group analyses (Zuo et al., 2010). For the Z-standardization, we normalized the ALFF value for each voxel by subtracting the global mean of the ALFF value and then the value was divided by the standard deviation (Yan et al., 2016).

ALFF analysis.

Individual standardized ALFF maps were implemented in a full-factorial ANCOVA model in SPM12 to examine the ALFF differences between HC, HIV, and PD groups in each of the four specific frequency bands. Independent groups (HC, HIV, and PD) and dependent frequency bands (LF, MF1, MF2 and HF) were modeled as factors. The frame-wise displacement value of each subject was modeled as a covariate to control for residual motion in the group analysis. To examine the sole impact of disease on frequency amplitude, age was also modeled as a covariate. An explicit gray matter mask was applied to the model. First, frequency difference regardless of disease were explored over all 99 subjects with the

contrasts specified between the four frequency bands (LF versus M1, LF versus M2, LF versus HF, M1 versus M2, M1 versus HF, M2 versus HF). Secondly, in the full-factorial ANCOVA model in SPM12, paired group-difference contrasts were specified for HC versus HIV, HC versus PD, and HIV versus PD (SPM *t*-contrasts) to examine whether ALFF values in each frequency band were greater or lesser between the three groups. Small volume correction analyses were applied to these t-contrasts to examine subcortical regions (caudate, putamen, pallidum, thalamus, amygdala, and hippocampus) using subcortical masks, generated based on Automated Anatomical Labeling template (Tzourio-Mazoyer et al., 2002). For further disease characteristics and brain-behavior relationships analyses, regional ALFF values were extracted from the clusters showing significant group differences using the MarsBaR ROI toolbox (http://marsbar.sourceforge.net/) implemented in SPM12. In addition, ALFF values of subcortical regions were also extracted irrespective of group using the subcortical masks.

Statistical significance for whole-brain ALFF analyses.

For statistical analysis of functional magnetic resonance imaging (fMRI) in SPM12, a high cluster-forming threshold *p*-value of 0.001 was set for each voxel in the whole brain maps, following recommended procedures (Woo et al., 2014; Roels et al., 2019). Significant clusters were then defined at a cluster threshold of $p<0.05$ corrected for multiple comparisons using false discovery rate (FDR), i.e., the proportion of activated voxels that are false positives. The small volume correction results were considered significant at an uncorrected significance threshold of $p<0.001$ and a peak-level threshold of $p<0.05$ corrected for family wise error (FWE) correction, i.e., the probability of one or more false positive voxels in the entire volume.

Statistical analyses of subcortical regions of interest.

Subcortical ALFF values, extracted from subcortical masks via the MarsBaR ROI toolbox irrespective of group, were subjected into SPSS (v.25, IBM, Armonk, NY, USA). MANCOVAs tested for group differences using group as between-subjects factor, frequency band as within-subject factor, age and motion as covariates.

Statistical analyses of brain-behavior relationships.

Partial correlation analyses were conducted in SPSS using age and motion as covariates to quantify the relationships between cognitive and motor performance with ALFF in subcortical and cortical brain regions for each group. Variables showing significant relationships were subjected to hierarchical multiple regression analyses controlling for age and motion in regression step 1, and estimating the contribution of regional ALFF power to performance in regression step 2. We used regression analyses to establish correlational relationships between multiple brain measures (brain regional ALFF values) and behavior (cognitive scores, clinical motor scores). ALFF-behavior correlation values between brain regions and test scores are presented in the regression tables, emphasizing the correlational nature of the analyses.

A statistical significance level was set at $p<0.05$, 2-tailed, for all tests unless stated otherwise. When applicable, Holm's Sequential Bonferroni Procedure was used to correct for multiple comparisons (Holm, 1979).

Results

Subcortical and cortical ALFF power characteristics

Over all subjects and independent of diagnosis, cortical regions showed greater oscillation power in the lower frequency domain, while subcortical regions showed greater oscillation power in the higher frequency domain (Figure 1). In particular, when comparing oscillation power between lower frequency (LF, M1) and higher frequency (M2, HF) bands, irrespective of group, cortical regions including the posterior (occipital, parietal lobules, angular, supramarginal gyrus, precuneus, and posterior cingulate cortex), sensorimotor, and prefrontal cortices (dorsolateral and medial prefrontal regions) showed greater frequency fluctuation power in the lower frequency domain (blue-green colors in Figure 1b, 1c, 1d, 1e). By contrast, subcortical regions including the BG (caudate head, pallidum, and putamen) and limbic system (amygdala, hippocampus, parahippocampus, insula, anterior temporal lobules, and anterior cingulate cortex) showed greater oscillation power in the higher frequency domains (yellow-red colors in Figure 1b, 1c, 1d, 1e). Minor differences in ALFF were observed between the LF and M1 bands (Figure 1a). The LF band showed greater ALFF in the temporal lobules, orbitofrontal gyrus (OFG), rectus, and premotor regions, while the M1 band had greater ALFF in the subcortical regions (amygdala, putamen, and thalamus), posterior insula, precuneus, and cingulate cortex (Figure 1a). Comparing M2 with HF, higher M2 ALFF was observed in cortical regions including the posterior, middle frontal, inferior frontal, sensorimotor cortical regions, insula, cingulate cortex, and thalamus, while HF showed greater power in the OFG, rectus, hippocampus, parahippocampus, and caudate (Figure 1f). It is worth noting that the thalamus showed highest ALFF power in the M1 band (Figure 1a, 1d, and 1e).

Between group analyses: Subcortical ALFF

To test the hypothesis that *subcortical* ALFF alterations occur with chronic HIV infection and similar to PD, we used MANCOVAs examining between-group differences in the extracted ALFF power for each subcortical region and frequency band with age and motion as covariates (Figure 2).

Basal ganglia.—The *putamen* group effect was marginally significant ($F(8,184)= 1.89$, $p=0.066$) with differences observed in the low (LF $F(2,94)=4.47$, $p=0.014$; $\eta_p^2=09$; observed power=.75) and the high frequency bands (HF $F(2,94)=3.9$, $p=0.024$; $\eta_p^2=.08$; observed power=.69). Follow-up pairwise group comparisons revealed that the PD group differed from the HC group (LF $p=0.008$, Cohen's $d=.71$) and the HIV group (LF $p=0.017$, Cohen's $d=.63$; HF $p=0.007$, Cohen's $d=.80$), while the HIV group did not differ from the HC group (p's>0.05). The overall *pallidum* group effect was marginally significant ($F(8,184)= 1.88$, $p=0.065$) with group differences in all frequency bandwidths (all p's<0.05; η_p^2 between .07 and .10; observed power between .67 and .83). Follow-up pairwise group comparisons showed that the PD group differed from the HC group in LF, M1, and M2 bands (p's<0.05,

Cohen's *d*'s=.68, .55, and .45, respectively) and from the HIV group in all four frequency bands (LF, M1, and M2 *p*'s<0.05, Cohen's *p*'s=.59, .71, and .63, respectively; HF *p*=0.002, Cohen's *d*=.88), while the HIV group did not differ from the HC group (*p*'s>0.05). No significant group differences were observed for the caudate ($F(8,184)=1.09$, $p=0.4$) or the thalamus ($F(8,184)=1.03$, $p=0.4$).

Limbic regions.—The *hippocampus* group effect was significant ($F(8,184)=2.49$, $p=0.014$) with differences in the middle and high frequency bands M1 ($F(2,94)=3.55$, $p=0.033$; $\eta_p^2=.07$; observed power=.65), M2 ($F(2,94)=8.43$, $p<0.0001$; $\eta_p^2=.15$; observed power=.96), and HF ($F(2,94)=3.58$, $p=0.038$; $\eta_p^2=.07$; observed power=.63). Pairwise group comparisons revealed that the PD group differed from the HC group (M2 $p=0.026$, Cohen's $d=.54$) and the HIV group (M1 $p=0.009$, Cohen's $d=.70$; M2 $p<0.0001$, Cohen's $d=.72$; HF $p=0.011$, Cohen's $d=.69$), while the HIV group did not differ from the HC group (*p*'s>0.05). No significant group difference in ALFF was observed for the amygdala ($F(8,184)=0.57$, $p=0.8$).

Whole brain ALFF

To test the hypothesis that ALFF alterations occur in the *whole brain* with chronic HIV infection and similar to Parkinson's disease, we used a full-factorial ANCOVA with groups and frequency bands as factors, as implemented in SPM12 for fMRI analysis. Overall, significant group differences in the low frequency band occurred mainly in cortical regions. Group effects in the middle and high frequency bands were observed in posterior cortical regions, hippocampus, and the cerebellum. Table 2 and Figure 3 illustrate the results for each frequency band, described in detail below.

LF oscillation power.—Within the *LF band* (Figure 3, upper panel, compared to HC participants, both HIV and PD patients (Table 2, LF, bold) showed significantly less frequency power in left frontal regions including the dorsolateral prefrontal cortex (dlPFC), medial prefrontal cortex (mPFC), and premotor cortical regions (BA6) (Figure 3, lower left panel: overlap HIV and PD). HIV patients further had significantly less LF power than HC participants in the bilateral inferior frontal gyrus (IFG) extending to the lower part of the premotor cortex (BA44/6), and less LF power in the left inferior parietal lobe (IPL; BA40). PD patients had significantly less LF power in the left putamen/pallidum relative to HC participants (Figure 3, upper left panel).

HIV patients showed significant higher LF oscillation power than HC participants and PD patients in sensorimotor regions (including supplementary motor area [SMA], paracentral, precentral and postcentral cortex; Figure 3, upper middle panel), right lingual cortex, inferior frontal regions (including bilateral OFG, rectus) as well as temporal regions (including the right inferior temporal gyrus [ITG], left superior temporal gyrus [STG], and Rolandic operculum [Rol. Oper.]) (Table 2, LF).

PD patients showed significantly higher LF oscillation power than both HC participants and HIV patients in the middle occipital gyri (MOG), and significantly higher LF power than HC participants in the OFG/rectus (Figure 3, upper right panel). PD patients further showed

lower LF power than HIV patients in the insula extending to the putamen (Figure 3, upper middle panel) (Table 2, LF).

M1 oscillation power.—Similar to LF, within *the M1 frequency band*, HIV patients showed significantly higher M1 power than HC participants in the right ITG. PD patients showed significantly higher M1 power than both HC and HIV participants in the MOG (Figure 3, lower middle panel) (Table 2, M1).

M2 and HF oscillation power.—In the higher frequency bands (M2 and HF), PD patients showed the least frequency power in the cerebellum compared to both HIV patients and HC participants. PD patients also showed less M2 power than HIV patients in the right hippocampus (Figure 3, lower right panel) (Table 2, M2 and HF).

Small Volume Correction analyses.—Compared to PD patients, HIV patients showed higher hippocampus ALFF values within the LF, M1 and M2 bands. In addition, HIV patients had greater ALFF power than PD patients in putamen and pallidum within LF and HF (Table 2, LF, M1, and M2).

Within group analyses: Relationship to age

Basal ganglia.—In HIV patients, older age was related to higher pallidal and thalamic ALFF power in the higher frequency bands (pallidum M2 r=.54, $p_{corrected}$=0.008; pallidum HF: r=.54, $p_{corrected}$=0.009; thalamus HF: r=.63, $p_{corrected}$<0.0001). The pallidum correlation was confirmed with the pallidum cluster from the whole brain analyses (HF: r=.53, p=0.003). No significant age effects for the BG were observed in the HC and PD groups.

Limbic regions.—In controls, older age correlated with higher hippocampal ALFF power (LF r=.40, $p_{corrected}$=0.044; M2 r=.60, $p_{corrected}$<0.0001; HF r=.49, $p_{corrected}$=0.015), In PD patients, older age was correlated with higher hippocampal ALFF power in the M2 frequency band (M2 r=.46, $p_{corrected}$=0.024). No significant age effects for subcortical limbic regions were observed in the HIV group.

Relationship to disease factors

Disease duration.—In the HIV group, the enhanced left inferior temporal gyrus LF power correlated with longer disease duration (r=.42, p=0.025). Higher LF power in this region also correlated with longer disease duration in the PD group (r=.35, p=0.044). Longer disease duration in PD patients further correlated with lower putamen M1 power (r=.35, p=0.043).

Peripheral immune markers.—Lower $CD4^+$ nadir values correlated moderately with lower pallidum (r=.48, p=0.020) and cerebellar (r=.44, p=0.037) oscillation power in the M2 bandwidth. Congruently, $CD4^+$ T cell counts at the time of the visit were also related to lower M2 pallidum ALFF power (r=.40, p=0.042; Figure 4). In comparison, PD patients had shown low M2 pallidal power.

LEDD.—Higher LEDD was moderately related to lower LF power in the right middle insula/putamen region (r=−.36, p=0.038).

Relationship to performance

These brain alterations are a neural correlate of behavior, such that more brain signal aberration would be related to more aberration in behavior, i.e., poorer cognitive and/or motor functioning.

Parkinsonian motor symptoms (UPDRS-III).—In the HIV group (Table 3A), the amygdala and thalamus M1-ALFF together explained thirty-one percent of the motor performance variance, with both contributing as significant independent predictors. These two variables also predicted twenty-six percent of the bradykinesia variance in the HIV group (F(2,22)=4.59, p=0.02).

In the PD group (Table 3B) on-dopaminergic medication, thirty-four percent of clinical motor symptoms were explained by motor/premotor, SMA, and occipital ALFF power, although only SMA power was a significant independent predictor. Forty-seven percent of motor symptoms off-dopaminergic medication were explained by striatal (caudate) HF-ALFF, and precentral/premotor and occipital LF-ALFF, with all three regions contributing as significant independent predictors.

Ataxia (SARA).—In the HIV group (Table 3A), the amygdala (M1), thalamus (LF), left middle frontal region (LF), and bilateral cerebellar ALFF together explained forty-three percent of the ataxia variance, with the amygdala and thalamus ALFF contributing as significant independent predictors.

In the PD group (Table 3B) on-dopaminergic medication, forty-eight percent of ataxia was explained by LF-ALFF in the putamen, motor/premotor, and prefrontal ALFF, with only the frontal regions contributing as significant independent predictors. Ataxia tested off-dopaminergic medication was to sixty percent explained by the putamen (LF), thalamus (M2), hippocampal (M1), prefrontal and occipital (MOG; LF) ALFF, with the thalamus, putamen, and hippocampus contributing as significant independent predictors.

Cognition.—In the HIV group (Table 4A), fifty percent of global cognitive ability (DRS-2 total score) was explained by high frequency (M2 and HF) ALFF in the striatum (caudate, putamen) and LF-ALFF in hippocampal, orbitofrontal, parietal, and occipital regions. Sixty-two percent of information processing speed (SDMT) was explained by LF-ALFF in limbic regions (amygdala, hippocampus), supplementary motor, temporal, and occipital regions in the HIV group, with the hippocampal and temporal regions contributing as significant independent predictors. Thirty-two percent of executive function deficit (Stroop-CW) was explained by putamen (M1), thalamus (LF), and inferior temporal (LF and M1) ALFF, with only the putamen contributing as a significant independent predictor. Twenty-nine percent of attention (digit span forward) was explained by LF hippocampus and IPL ALFF. Sixteen percent of immediate memory (IM; CVLT-II) was explained by inferior parietal LF-ALFF. Forty-one percent of long-delay memory (LD; CVLT-II) was explained by pallidal (M1),

hippocampal (LF), orbitofrontal (LF), and occipital (LF) ALFF, with only the pallidum contributing as significant independent predictor.

In the PD group (Table 4B), thirty percent of global cognitive skill was explained by LF limbic (amygdala, hippocampus) ALFF. Twenty-seven percent of information processing speed was explained by amygdala (M1) and bilateral OFG (LF) ALFF, with each contributing as significant independent predictors. M1 amygdala ALFF also explained nine percent of the executive control (Stroop-CW) variance, for which age was the main predictor in the model. Executive control with high working memory load (Digit Span Backward) was to twenty-two percent explained by M2 hippocampal and LF left IPL ALFF. Twenty-one percent of immediate memory (CVLT-IM) was explained by amygdala (M1 and M2) ALFF. Forty-one percent of long-delay memory (CVLT-LD) was explained by striatal (HF caudate, LF putamen) and occipital (LF) ALFF, with only the caudate contributing as a significant independent predictor. Finally, thirty-two percent of the visuospatial performance (JLO) deficit in the PD group was explained by striatal (M2 caudate, LF putamen) and hippocampal (LF and M2) ALFF.

Discussion

To better understand the pathogenesis and heterogeneity of neurocognitive functioning in older virally-controlled HIV patients on ART, we examined the subcortical and cortical oscillation power dynamics in this cohort and compared them to those with age-related neurodegenerative PD and healthy aging controls. Altered ALFF power dynamics occurred in several brain regions supporting the assumption of brain functional compromise in HIV patients despite ART (Chaganti et al., 2017). Essentially, older HIV patients showed abnormalities in cortical power dynamics with decreased frontal and enhanced sensorimotor and temporal low-frequency oscillation power consistent with a shift toward more cortical than subcortical involvement as suggested by Heaton and colleagues (Heaton et al., 2011) for disease progression in the post-ART era. ALFF aberrations in sensorimotor areas were a dominant HIV-specific feature and consistent with a previous report by Bak et al. (2018) where it differentiated HAND from cognitively unimpaired HIV individuals. Other neuroimaging studies also found aberrant neural activity in these cortical regions in HIV (Chaganti et al., 2017) and particularly sensorimotor areas (Becker et al., 2011), suggesting it may be a substrate for sensorimotor problems.

Similarities between HIV and PD group were observed in overlapping frontal hypoactivation patterns that were significantly different from controls in both groups. The attenuated prefrontal activity in PD occurred together with enhanced occipital ALFF values. Decreased frontal cortical ALFF within the motor circuit (Hu et al., 2015; Li et al., 2017; Wang et al., 2018) has been previously linked to dopamine availability (Kwak et al., 2012) and the pathogenesis of non-motor symptoms in PD (Li et al., 2017). We now show that alterations in the intrinsic ALFF power dynamics in this BG-thalamic-cortical circuitry included occipital cortical oscillation power dynamics in PD. These same power dynamics were associated with cognitive ability across several domains in the older HIV cohort, which is corroborated by a task-activated fMRI study that showed prefrontal and caudate

hypoactivation together with posterior hyperactivation that preceded the development of cognitive impairment in HIV (Melrose et al., 2008).

The profile of subcortical frequency fluctuations of the BOLD signal offered an additional characterization to further understand the neurocognitive heterogeneity that occurs with aging influenced by HIV infection. Subcortical BG regions have been regarded as susceptible to HIV-1 replication (Stout et al., 1998; Kumar et al., 2011) and synaptodendritic injury even with ART (Schier et al., 2017)—alterations in regions that are implicated in the hallmark motor symptoms in PD (Moustafa et al., 2016). We accordingly assessed BG ALFF power dynamics in HIV and PD across all frequency bandwidths, and particularly higher frequencies that are sensitive to BOLD fluctuation in subcortical regions (e.g., Baria et al., 2011). Consistent with the hypothesis of decreased dopaminergic function (for a meta-analysis see Pan et al., 2017) and previous reports of reduced BG ALFF in PD (striatum: Li et al., 2017; pallidum: Wang et al., 2018), PD patients in our cohort exhibited reduced pallidum amplitudes. Although BG-ALFF did not significantly differ between the HIV group and controls, HIV patients demonstrated heterogeneity in neural oscillation dynamics that may be explained by immune system compromise. HIV patients with lower $CD4^+$ nadir values and $CD4^+$ T cell counts at the time of the visit had lower pallidum oscillation power in the higher M2 frequency band. Without direct knowledge about potentially persisting neuroinflammation in the brain (Ferguson et al., 2016), this may be an indirect sign that the virus affects the BG at a neurofunctional level depending on disease severity as tracked by $CD4^+$ T cell counts. That both $CD4^+$ nadir values and $CD4^+$ T cell counts were associated with lower pallidal frequency power (although they were not significantly related to each other) raises the question of whether persistent immune activation leading to $CD4^+$ T cell depletion in the acute phase of the disease (past insult; $CD4^+$ nadir) affects ALFF more permanently, while temporary activation of the immune system (without immune exhaustion) with ART alters intrinsic brain signal oscillations more transiently, and can be restored with treatment and adherence. Corroborating our results, Li et al. (2019) reported BG ALFF abnormalities in the striatum in recently infected HIV patients, a result that was supported by animal studies on acute HIV effects on striatal ALFF (Zhao et al., 2019). A longitudinal human morphological study (Stout et al., 1998) additionally showed caudate atrophy during the early stages of the disease that was accelerated during advanced illness. However, neurofunctional frequency power aberrations in striatal regions (caudate, putamen) were not significant in our cohort at the group level in chronic HIV-infected individuals. Across the literature, there is a broad heterogeneity in the neural systems affected among HIV-positive patients associated with disparate disease progression. For example, motor alterations in HIV-positive patients have been associated with degeneration of the nigrostriatal system (Berger and Arendt, 2000; Khanlou et al., 2009) and ponto-cerebellar pathways (Sullivan et al., 2011), as well as neurocognitive impairments with neural degeneration of neocortex and mesolimbic hippocampal pathways (e.g., Hakkers et al., 2017). Here, in older HIV-infected individuals, this variability in cognitive and motor abilities was related to ALFF abnormalities spanning these brain systems.

Over the course of the disease, subcortical ALFF alterations may fluctuate with immune health and contribute to the observed heterogeneity of neurocognitive and motor compromise and disease progression among people living with HIV infection long-term

(Grant et al., 2014; Sacktor et al., 2016). Collectively, intrinsic neurofunctional ALFF characteristics of BG and cortical regions may serve as a marker of HIV effects on the brain (for an animal model, see Lee et al., 2014), possibly via HIV-associated dopaminergic abnormalities (Chang et al., 2004; Wang et al., 2004; Kumar et al., 2011) that bear similarities to the frontostriatal circuit dysfunction in PD during tasks (Lewis et al., 2003) and at rest (Baggio et al., 2015). To our knowledge, this is the first study to show that ALFF can capture neurofunctional abnormalities in an older, chronically treated HIV cohort, and in comparison, showing some similarities in ALFF characteristics to PD pathophysiology.

As reported previously in healthy (Zuo et al., 2010; Baria et al., 2011) and clinical samples (Hong et al., 2018), the organization of the resting brain is such that cortical regions have a LF oscillation preference supporting long-distance communication across cortical regions, while subcortical regions oscillate at higher frequencies for communicating among closely localized BG and other subcortical nodes including limbic and cerebellar regions. The brain may use these frequency-specific channels of communication to convey behaviorally relevant information (Zavala et al., 2014). Our data suggest that disruption of these neural frequency dynamics in subcortical-cortical circuitry could contribute to the development of cognitive and motor dysfunction across disorders. ALFF dynamics across different frequency bands largely correlated with interindividual differences in cognitive and motor performances in the HIV and PD groups. For example, subcortical and cortical ALFF explained over 50% of global cognitive ability, which included the striatum (caudate, putamen), hippocampus, orbitofrontal, parietal, and occipital regions. Motor dysfunction (UPDRS and ataxia) in PD was explained up to 60% by ALFF in the motor circuit (caudate, putamen, precentral/premotor cortex), dlPFC, limbic, and occipital regions. Interindividual differences in motor performance in the HIV group, particularly ataxia, were also over 50% explained by ALFF power dynamics in the motor circuit (thalamus, precentral/premotor cortex, and cerebellum) and the amygdala. As a cautionary note, explanatory power as in regression analyses is not causality, and it cannot be implied that brain signal aberration causes aberration in behavior. In fact, the underlying cause of both brain signal aberration and aberration in behavior is presumably the disease state.

Subcortical limbic regions, in particular the hippocampus, are sensitive to the effects of aging (Oren et al., 2019). Consistent with the assumption of an age-HIV interaction, Guha et al. (2016) showed that elderly HIV-infected individuals (>60 years) with detectable plasma HIV viral load (compared to those with undetectable viral load) had decreased functional connectivity in the salience network, a network that connects the amygdala, thalamus, and specific brainstem nuclei and integrates emotional value to neural systems (Seeley, 2019). Thus, age-related limbic ALFF dynamics may add to disease-specific effects. In both the HIV and PD groups, hippocampus and amygdala ALFF values contributed to explaining the cognitive performance variance. In HIV patients, hippocampal and amygdala ALFF was specifically associated with slowed processing speed, which had been attributed to BG involvement in the pre-ART era (Heaton et al., 2011). With increased efficiency of ART, many HIV-infected individuals are virologically suppressed and the BG insult may be less pronounced, and vary with immune status and immunosenescence in older cohorts. For example, older age correlated with hippocampal frequency dynamics in the HC and PD groups consistent with the literature (e.g., Oren et al., 2019), and with putamen and thalamus

power dynamics in HIV patients. Thus, older age, HIV chronicity, immune health and ART affect subcortical ALFF power dynamically and likely add to interindividual differences in disease phenotypes (Rubin et al., 2018) and progression.

A limitation of this study is that it is cross-sectional and cannot address the question of brain function damage progression over the course of HIV infection despite ART. Our correlational findings denote pronounced HIV-specific inferior temporal gyrus ALFF aberration (that was associated with executive dysfunction) with longer disease duration. The question remains whether altered ALFF power dynamics are due to continued neuroinflammation (Ferguson et al., 2016) or have accumulated in the aging brain, as has been suggested by others considering that many antiretroviral drugs did not effectively penetrate the blood brain barrier (Ellero et al., 2017). We have, however, some indirect indication that HIV disease severity affects the motor circuity in older HIV individuals on ART established via correlational relationships between $CD4^+$ T cell counts and pallidum and cerebellar ALFF alterations that were in the direction of the neural frequency oscillation power deficit in PD.

In summary, our study revealed disease-specific neurofunctional aberrations in HIV and PD patients (relative to controls) in cortical, subcortical, and cerebellar regions across all frequency bands. Importantly and in line with our assumption, abnormalities in cortical BOLD oscillations were related to cognitive and motor ability, together with ALFF power variations in subcortical limbic-striatal regions. ALFF shows promise for furthering our understanding of the pathogenesis of motor disturbances and cognitive compromise in older virally-controlled HIV patients on ART and could serve as a biomarker for neurocognitive compromise and disease progression across disorders.

Supplementary Material

Refer to Web version on PubMed Central for supplementary material.

Acknowledgements

We thank Ryan Goodcase, Joshua Karpf, Ember Kalon, Eden Gallanter, Priya Asok, and Stephanie Sassoon for assistance with recruitment, screening, clinical interviewing, and testing of study participants, Weiwei Chu for assistance with data management, and Adolf Pfefferbaum for comments on the manuscript.

Funding

This work was supported by the National Institute on Alcohol Abuse and Alcoholism (AA023165, AA017347, AA017168), National Institute on Neurological Disorders and Stroke (NS075097), National Institute on Aging (AG047366), and the Michael J Fox Foundation for Parkinson’s Research.

References

Baggio HC, Segura B, Junque C (2015) Resting-state functional brain networks in Parkinson’s disease. CNS neuroscience & therapeutics 21:793–801. [PubMed: 26224057]

Bak Y, Jun S, Choi JY, Lee Y, Lee SK, Han S, Shin NY (2018) Altered intrinsic local activity and cognitive dysfunction in HIV patients: A resting-state fMRI study. PloS one 13:e0207146. [PubMed: 30496203]

Baria AT, Baliki MN, Parrish T, Apkarian AV (2011) Anatomical and functional assemblies of brain BOLD oscillations. J Neurosci 31:7910–7919. [PubMed: 21613505]

Becker JT, Sanders J, Madsen SK, Ragin A, Kingsley L, Maruca V, Cohen B, Goodkin K, Martin E, Miller EN (2011) Subcortical brain atrophy persists even in HAART-regulated HIV disease. Brain imaging and behavior 5:77–85. [PubMed: 21264551]

Benton AL, Hamsher K, Varney NR, Spreen O (1983) Judgment of line orientation: Oxford University Press New York.

Berger JR, Arendt G (2000) HIV dementia: the role of the basal ganglia and dopaminergic systems. J Psychopharmacol 14:214–221. [PubMed: 11106299]

Brew BJ, Crowe SM, Landay A, Cysique LA, Guillemin G (2009) Neurodegeneration and ageing in the HAART era. J Neuroimmune Pharmacol 4:163–174. [PubMed: 19067177]

Chaganti JR, Heinecke A, Gates TM, Moffat KJ, Brew BJ (2017) Functional Connectivity in Virally Suppressed Patients with HIV-Associated Neurocognitive Disorder: A Resting-State Analysis. AJNR Am J Neuroradiol 38:1623–1629. [PubMed: 28596187]

Chang L, Lee PL, Yiannoutsos CT, Ernst T, Marra CM, Richards T, Kolson D, Schifitto G, Jarvik JG, Miller EN, Lenkinski R, Gonzalez G, Navia BA, Consortium HM (2004) A multicenter in vivo proton-MRS study of HIV-associated dementia and its relationship to age. Neuroimage 23:1336–1347. [PubMed: 15589098]

Dauer W, Przedborski S (2003) Parkinson's disease: mechanisms and models. Neuron 39:889–909. [PubMed: 12971891]

Delis DC, Kramer J, Kaplan E, Ober BA (2000) CVLT-II: California verbal learning test: adult version: Psychological Corporation.

Ellero J, Lubomski M, Brew B (2017) Interventions for neurocognitive dysfunction. Current HIV/AIDS Reports 14:8–16. [PubMed: 28110422]

Esposito F, Tessitore A, Giordano A, De Micco R, Paccone A, Conforti R, Pignataro G, Annunziato L, Tedeschi G (2013) Rhythm-specific modulation of the sensorimotor network in drug-naive patients with Parkinson's disease by levodopa. Brain : a journal of neurology 136:710–725. [PubMed: 23423673]

Ferguson D, Clarke S, Berry N, Almond N (2016) Attenuated SIV causes persisting neuroinflammation in the absence of a chronic viral load and neurotoxic antiretroviral therapy. AIDS (London, England) 30:2439.

First M, Spitzer R, Gibbon M, Williams J (1998) Structured clinical interview for DSM-IV axis I disorders: patient edition (February 1996 final). In: SCID-I/P.

Fox MD, Raichle ME (2007) Spontaneous fluctuations in brain activity observed with functional magnetic resonance imaging. Nat Rev Neurosci 8:700–711. [PubMed: 17704812]

Galvan A, Devergnas A, Wichmann T (2015) Alterations in neuronal activity in basal ganglia-thalamocortical circuits in the parkinsonian state. Front Neuroanat 9:5. [PubMed: 25698937]

Gelb DJ, Oliver E, Gilman S (1999) Diagnostic criteria for Parkinson disease. Archives of neurology 56:33–39. [PubMed: 9923759]

Golden CJ (1978) Stroop color and word test: A manual for clinical and experimental uses. Chicago, IL: Stoelting.

Grant I et al. (2014) Asymptomatic HIV-associated neurocognitive impairment increases risk for symptomatic decline. Neurology 82:2055–2062. [PubMed: 24814848]

Guha A, Wang L, Tanenbaum A, Esmaeili-Firidouni P, Wendelken LA, Busovaca E, Clifford K, Desai A, Ances BM, Valcour V (2016) Intrinsic network connectivity abnormalities in HIV-infected individuals over age 60. Journal of neurovirology 22:80–87. [PubMed: 26265137]

Hakkers CS, Arends JE, Barth RE, Du Plessis S, Hoepelman AI, Vink M (2017) Review of functional MRI in HIV: effects of aging and medication. Journal of neurovirology 23:20–32. [PubMed: 27718211]

Heaton RK et al. (2010) HIV-associated neurocognitive disorders persist in the era of potent antiretroviral therapy: CHARTER Study. Neurology 75:2087–2096. [PubMed: 21135382]

Heaton RK et al. (2011) HIV-associated neurocognitive disorders before and during the era of combination antiretroviral therapy: differences in rates, nature, and predictors. Journal of neurovirology 17:3–16. [PubMed: 21174240]

Herzog J, Volkmann J, Krack P, Kopper F, Potter M, Lorenz D, Steinbach M, Klebe S, Hamel W, Schrader B, Weinert D, Muller D, Mehdorn HM, Deuschl G (2003) Two-year follow-up of

subthalamic deep brain stimulation in Parkinson's disease. Movement disorders : official journal of the Movement Disorder Society 18:1332–1337. [PubMed: 14639676]

Holm S (1979) A simple sequentially rejective multiple test procedure. Scandinavian journal of statistics:65–70.

Hong JY, Müller-Oehring EM, Pfefferbaum A, Sullivan EV, Kwon D, Schulte T (2018) Aberrant blood-oxygen-level-dependent signal oscillations across frequency bands characterize the alcoholic brain. Addiction biology 23:824–835. [PubMed: 28699704]

Hu XF, Zhang JQ, Jiang XM, Zhou CY, Wei LQ, Yin XT, Li J, Zhang YL, Wang J (2015) Amplitude of low-frequency oscillations in Parkinson's disease: a 2-year longitudinal resting-state functional magnetic resonance imaging study. Chin Med J (Engl) 128:593–601. [PubMed: 25698189]

Jurica P, Leitten C, Mattis S (2004) DRS-2 dementia rat-630 ing scale-2: Professional manual. Psychological Assessment 631.

Khanlou N, Moore DJ, Chana G, Cherner M, Lazzaretto D, Dawes S, Grant I, Masliah E, Everall IP, Group H (2009) Increased frequency of alpha-synuclein in the substantia nigra in human immunodeficiency virus infection. Journal of neuro virology 15:131–138. [PubMed: 19115126]

Kumar AM, Ownby RL, Waldrop-Valverde D, Fernandez B, Kumar M (2011) Human immunodeficiency virus infection in the CNS and decreased dopamine availability: relationship with neuropsychological performance. Journal of neuro virology 17:26–40. [PubMed: 21165787]

Kwak Y, Peltier S, Bohnen N, Müller M, Dayalu P, Seidler RD (2012) L-DOPA changes spontaneous low-frequency BOLD signal oscillations in Parkinson's disease: a resting state fMRI study. Frontiers in systems neuroscience 6:52. [PubMed: 22783172]

Lee DE, Reid WC, Ibrahim WG, Peterson KL, Lentz MR, Marie D, Choyke PL, Jagoda EM, Hammoud DA (2014) Imaging dopaminergic dysfunction as a surrogate marker of neuropathology in a small-animal model of HIV. Molecular imaging 13:7290.2014. 00031.

Lewis SJ, Dove A, Robbins TW, Barker RA, Owen AM (2003) Cognitive impairments in early Parkinson's disease are accompanied by reductions in activity in frontostriatal neural circuitry. Journal of Neuroscience 23:6351–6356. [PubMed: 12867520]

Li D, Huang P, Zang Y, Lou Y, Cen Z, Gu Q, Xuan M, Xie F, Ouyang Z, Wang B, Zhang M, Luo W (2017) Abnormal baseline brain activity in Parkinson's disease with and without REM sleep behavior disorder: A resting-state functional MRI study. J Magn Reson Imaging 46:697–703. [PubMed: 27880010]

Li R, Wang W, Wang Y, Peters S, Zhang X, Li H (2019) Effects of early HIV infection and combination antiretroviral therapy on intrinsic brain activity: a cross-sectional resting-state fMRI study. Neuropsychiatr Dis Treat 15:883–894. [PubMed: 31114203]

Litvan I, Goldman JG, Troster AI, Schmand BA, Weintraub D, Petersen RC, Mollenhauer B, Adler CH, Marder K, Williams-Gray CH, Aarsland D, Kulisevsky J, Rodriguez-Oroz MC, Bum DJ, Barker RA, Emre M (2012) Diagnostic criteria for mild cognitive impairment in Parkinson's disease: Movement Disorder Society Task Force guidelines. Movement disorders : official journal of the Movement Disorder Society 27:349–356. [PubMed: 22275317]

MDS-UPDRS (2003) Movement Disorder Society Task Force on Rating Scales for Parkinson's Disease. The unified Parkinson's disease rating scale (UPDRS): status and recommendations. Movement Disorders 18:738–750. [PubMed: 12815652]

Melrose RJ, Tinaz S, Castelo JM, Courtney MG, Stern CE (2008) Compromised frontostriatal functioning in HIV: an fMRI investigation of semantic event sequencing. Behav Brain Res 188:337–347. [PubMed: 18242723]

Morgan EE, Iudicello JE, Weber E, Duarte NA, Riggs PK, Delano-Wood L, Ellis R, Grant I, Woods SP, Group HIVNRP (2012) Synergistic effects of HIV infection and older age on daily functioning. J Acquir Immune Defic Syndr 61:341–348. [PubMed: 22878422]

Moustafa AA, Chakravarthy S, Phillips JR, Gupta A, Keri S, Polner B, Frank MJ, Jahanshahi M (2016) Motor symptoms in Parkinson's disease: A unified framework. Neuroscience & Biobehavioral Reviews 68:727–740. [PubMed: 27422450]

Oren N, Ash E, Shapira-Lichter I, Elkana O, Reichman-Eisikovits O, Chomsky L, Lerner Y (2019) Changes in resting-state functional connectivity of the hippocampus following cognitive effort

predict memory decline at the older age–a longitudinal fMRI study. Frontiers in aging neuroscience 11:163. [PubMed: 31379554]

Pan P, Zhan H, Xia M, Zhang Y, Guan D, Xu Y (2017) Aberrant regional homogeneity in Parkinson's disease: a voxel-wise meta-analysis of resting-state functional magnetic resonance imaging studies. Neuroscience & Biobehavioral Reviews 72:223–231. [PubMed: 27916710]

Power JD, Schlaggar BL, Petersen SE (2015) Recent progress and outstanding issues in motion correction in resting state fMRI. Neuroimage 105:536–551. [PubMed: 25462692]

Roels SP, Loeys T, Moerkerke B (2019) Including Data Analytical Stability in Cluster-based Inference. bioRxiv:844860.

Rubin LH, Sacktor N, Creighton J, Du Y, Endres CJ, Pomper MG, Coughlin JM (2018) Microglial activation is inversely associated with cognition in individuals living with HIV on effective antiretroviral therapy. AIDS 32:1661–1667. [PubMed: 29746297]

Sacktor N, Skolasky RL, Seaberg E, Munro C, Becker JT, Martin E, Ragin A, Levine A, Miller E (2016) Prevalence of HIV-associated neurocognitive disorders in the Multicenter AIDS Cohort Study. Neurology 86:334–340. [PubMed: 26718568]

Schier CJ, Marks WD, Paris JJ, Barbour AJ, McLane VD, Maragos WF, McQuiston AR, Knapp PE, Hauser KF (2017) Selective vulnerability of striatal D2 versus D1 dopamine receptor-expressing medium spiny neurons in HIV-1 tat transgenic male mice. Journal of Neuroscience 37:5758–5769. [PubMed: 28473642]

Schmitz-Hübsch T, Du Montcel ST, Baliko L, Berciano J, Boesch S, Depondt C, Giunti P, Globas C, Infante J, Kang J-S (2006) Scale for the assessment and rating of ataxia: development of a new clinical scale. Neurology 66:1717–1720. [PubMed: 16769946]

Seeley WW (2019) The salience network: a neural system for perceiving and responding to homeostatic demands. Journal of Neuroscience.

Smith A (1973) Digit symbol modalities test. Los Angeles: Western Psychological Services.

Smith A (1982) Digit symbol modalities test (SDMT) manual [revised]. Los Angeles: Western Psychological Services.

Stout JC, Ellis RJ, Jernigan TL, Archibald SL, Abramson I, Wolfson T, McCutchan JA, Wallace MR, Atkinson JH, Grant I (1998) Progressive cerebral volume loss in human immunodeficiency virus infection: a longitudinal volumetric magnetic resonance imaging study. Archives of neurology 55:161–168. [PubMed: 9482357]

Sullivan EV, Rosenbloom MJ, Rohlfing T, Kemper CA, Deresinski S, Pfefferbaum A (2011) Pontocerebellar contribution to postural instability and psychomotor slowing in HIV infection without dementia. Brain Imaging Behav 5:12–24. [PubMed: 20872291]

Tesic T, Boban J, Bjelan M, Todorovic A, Kozic D, Brkic S (2018) Basal ganglia shrinkage without remarkable hippocampal atrophy in chronic aviremic HIV-positive patients. Journal of neurovirology 24:478–487. [PubMed: 29687405]

Tzourio-Mazoyer N, Landeau B, Papathanassiou D, Crivello F, Etard O, Delcroix N, Mazoyer B, Joliot M (2002) Automated anatomical labeling of activations in SPM using a macroscopic anatomical parcellation of the MNI MRI single-subject brain. Neuroimage 15:273–289. [PubMed: 11771995]

van Sighem AI, Gras LA, Reiss P, Brinkman K, de Wolf F, study Anoc (2010) Life expectancy of recently diagnosed asymptomatic HIV-infected patients approaches that of uninfected individuals. AIDS 24:1527–1535. [PubMed: 20467289]

Wang GJ, Chang L, Volkow ND, Telang F, Logan J, Ernst T, Fowler JS (2004) Decreased brain dopaminergic transporters in HIV-associated dementia patients. Brain : a journal of neurology 127:2452–2458. [PubMed: 15319273]

Wang J, Zhang JR, Zang YF, Wu T (2018) Consistent decreased activity in the putamen in Parkinson's disease: a meta-analysis and an independent validation of resting-state fMRI. Gigascience 7.

Wechsler D (1987) WMS-R: Wechsler memory scale-revised: Psychological Corporation.

Wechsler D (2001) Wechsler Test of Adult Reading: WTAR: Psychological Corporation.

Woo CW, Krishnan A, Wager TD (2014) Cluster-extent based thresholding in fMRI analyses: pitfalls and recommendations. Neuroimage 91:412–419. [PubMed: 24412399]

Yan CG, Wang XD, Zuo XN, Zang YF (2016) DPABI: Data Processing & Analysis for (Resting-State) Brain Imaging. Neuroinformatics 14:339–351. [PubMed: 27075850]

Zavala BA, Tan H, Little S, Ashkan K, Hariz M, Foltynie T, Zrinzo L, Zaghloul KA, Brown P (2014) Midline frontal cortex low-frequency activity drives subthalamic nucleus oscillations during conflict. Journal of Neuroscience 34:7322–7333. [PubMed: 24849364]

Zhao J, Chen F, Ren M, Li L, Li A, Jing B, Li H (2019) Low-frequency fluctuation characteristics in rhesus macaques with SIV infection: a resting-state fMRI study. Journal of neurovirology 25:141–149. [PubMed: 30478797]

Zou QH, Zhu CZ, Yang Y, Zuo XN, Long XY, Cao QJ, Wang YF, Zang YF (2008) An improved approach to detection of amplitude of low-frequency fluctuation (ALFF) for resting-state fMRI: fractional ALFF. J Neurosci Methods 172:137–141. [PubMed: 18501969]

Zuo XN, Di Martino A, Kelly C, Shehzad ZE, Gee DG, Klein DF, Castellanos FX, Biswal BB, Milham MP (2010) The oscillating brain: complex and reliable. Neuroimage 49:1432–1445. [PubMed: 19782143]

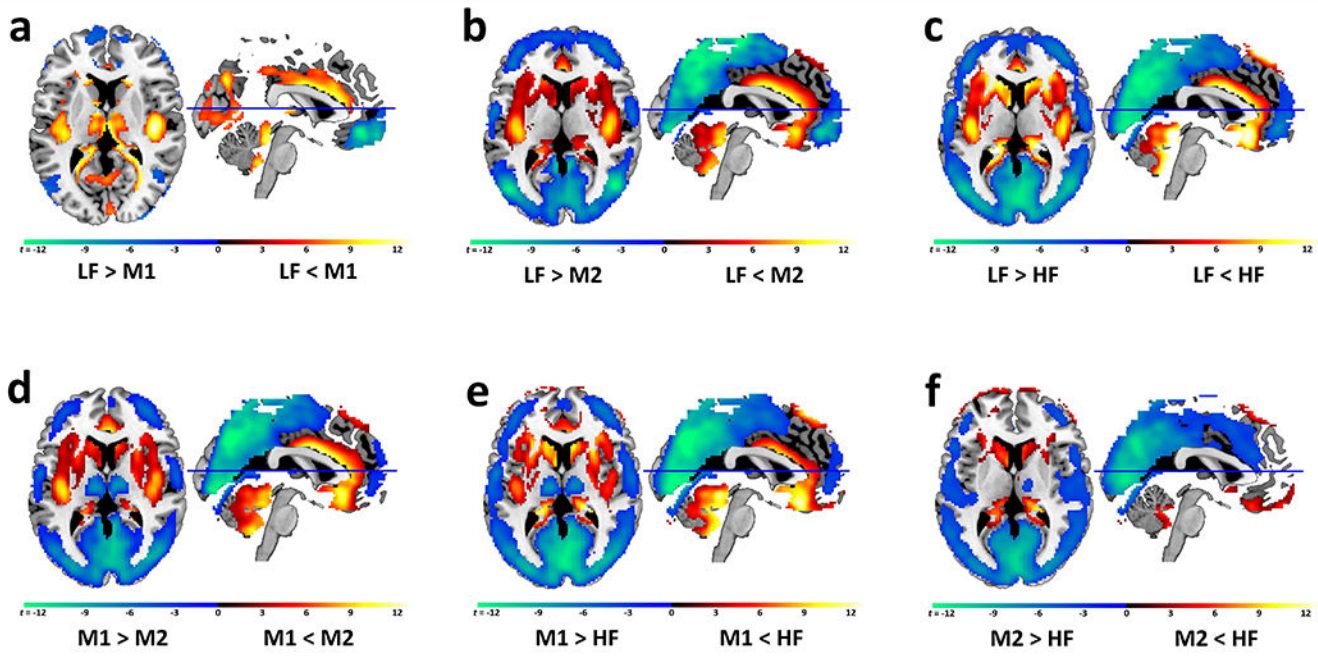

Figure 1. Brain ALFF distribution.

Subcortical and cortical frequency oscillation band preferences over all subjects independent of diagnosis.

Panels b, c, d, e: Cortical brain regions (green-blue) show higher ALFF values in the lower frequency (LF, M1) bands than in the higher frequency (M2, HF) bands, while subcortical brain regions (yellow-red) show higher ALFF values in the higher frequency (HF, M2) than the lower frequency (LF, M1) bands (panel b: LF versus M2; panel c: LF versus HF; panel d: M1 versus M2; panel e: M1 versus HF). Minor differences in ALFF power occurred among lower frequency bands, LF versus M1 (panel a), and among higher frequency bands, M2 versus HF (panel f). The thalamus is unique in that it shows higher ALFF values in the M1 frequency band than LF (panel a: M1>LF; yellow-red) and HF bands (panel d: M1>M2; panel e: M1>HF; green-blue).

Abbreviations: low frequency (LF) (0.01-0.027 Hz), middle frequency 1 (M1) (0.027-0.073 Hz), middle frequency 2 (M2) (0.073-0.17 Hz) and high frequency (HF) (0.17-0.25 Hz).

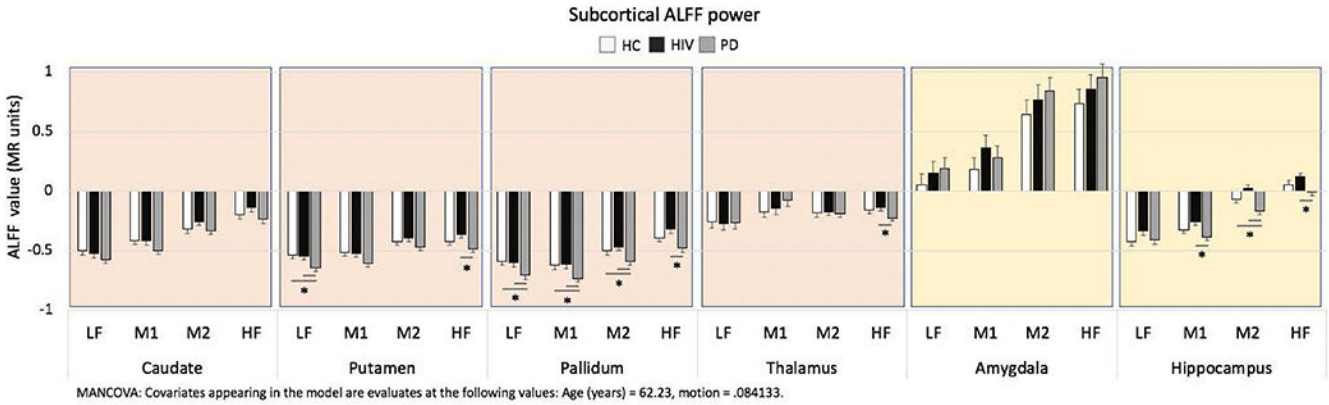

Figure 2. ALFF values for subcortical regions of interest - Between group analyses.

Bar graphs depict each group's average ALFF power and standard error.

MANCOVAs comparing study groups (PD, HIV, HC) for each frequency band (LF, M1, M2, HF) with age and motion as covariates, for each region; post-hoc LSD paired group comparisons, significance level $p<0.05$.

Significant pairwise group differences are indicated by an asterisk.

Abbreviations: Study groups by diagnosis: Healthy control (HC) group, HIV infection (HIV) group, Parkinson's disease (PD) group; oscillation frequency bands: low frequency (LF), middle frequency 1 (M1), middle frequency 2 (M2), high frequency (HF).

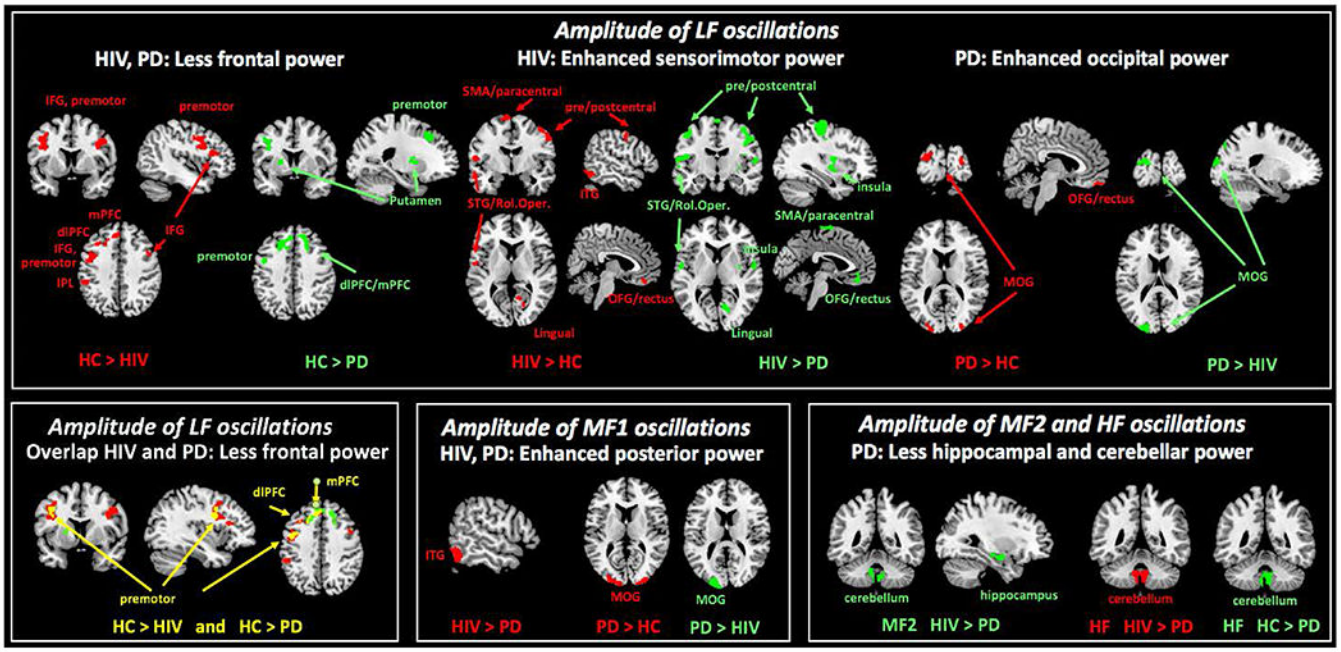

Figure 3. Study group comparison of whole brain ALFF values.

Results are depicted for paired group contrasts for each frequency band: lower frequency (LF; left panel), middle frequency (M1; upper right panel), and higher frequency bands (M2, HF; lower right panel). Full-factorial model in SPM12 with the between-subjects factor study groups by diagnosis (PD, HIV, HC), within-subject factor frequency band (LF, M1, M2, HF), and age and motion as covariates. Cluster significance threshold was set at $p<0.05$ corrected for multiple comparisons.

Abbreviations: Study groups by diagnosis: Healthy control (HC) group, HIV infection (HIV) group, Parkinson's disease (PD) group; oscillation frequency bands: low frequency (LF), middle frequency 1 (M1), middle frequency 2 (M2), high frequency (HF).

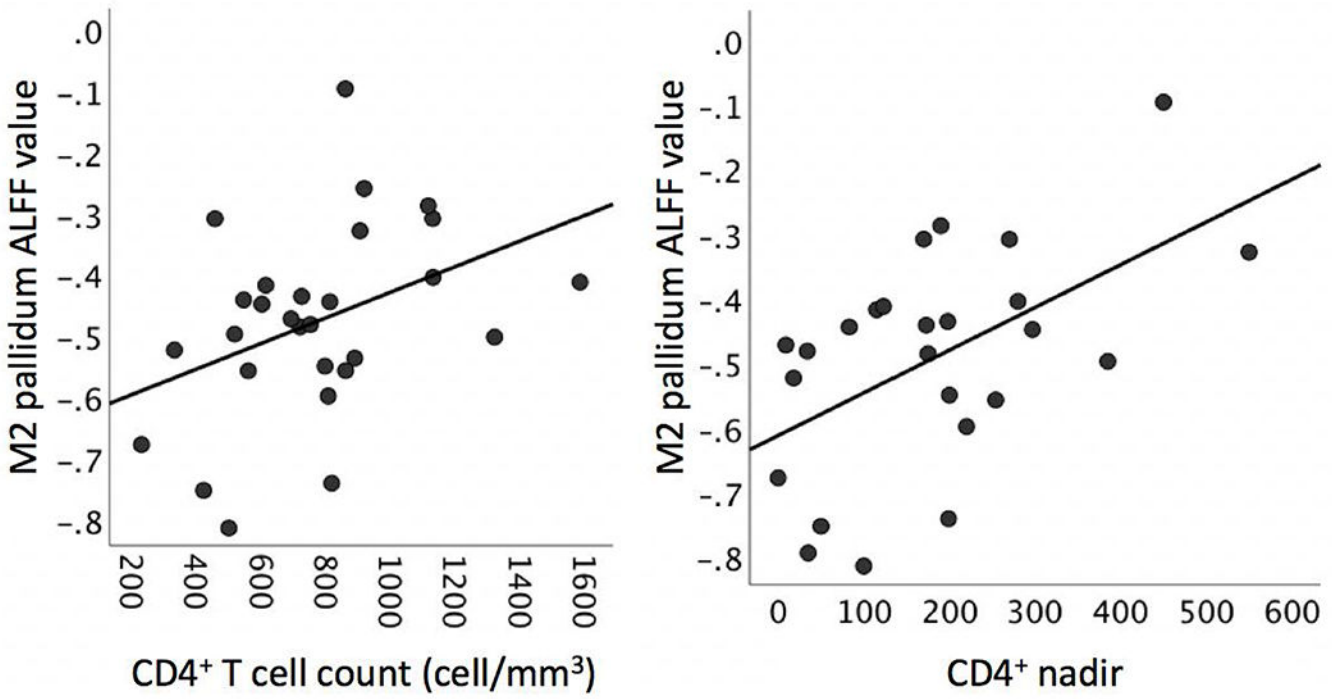

Figure 4. Peripheral immune system markers and pallidal M2-ALFF in HIV patients.

Left panel: $CD4^+$ T cell count at the time of the visit. Right panel: $CD4^+$ nadir (i.e., lowest $CD4^+$ value in an individual's disease history). $CD4^+$ nadir and $CD4^+$ T cell count were not significantly correlated with each other (r=.23, p>0.05).

Table 1:

Study sample characteristics

Diag.	N	Sex[1] m/w	Age (yrs)	Education (yrs)	SES	YSD (yrs)	Verbal IQ[2]	Global Cognition[2]
HC	33	15/18	61±10	16 ±2	22±10	-	114±10	140±3
HIV	30	19/11	60±7	14±2	38±15	26±8	100±19	138±5
PD	36	22/14	66±8	17±2	21±8	4±2	113±11	139±4
P		ns	*0.008*	*0.0001*	*0.0001*	*0.0001*	ns	ns
post-hoc			PD > HC, HIV	HC, PD > HIV	HIV > HC, PD	HIV > PD		

Group means ± standard deviations.

Abbreviations: Study groups by diagnosis (Diag.): Healthy control (HC) group, HIV infection (HIV) group, Parkinson's disease (PD) group; number of participants (N); men (m), women (w); years (yrs); socioeconomic status (SES): lower scores denote higher SES; years since diagnosis (YSD).

[1] χ^2 test; [2]MANCOVA with age and education as co-variates; statistical significance level (p), pairwise comparisons least significant difference (LSD) post-hoc test.

[2]Verbal intelligence quotient (IQ): Wechsler test of adult reading - standard score (WTAR-SS), Global cognition: Dementia Rating Scale 2nd edition (DRS-2).

Table 2.

Group differences in ALFF values within four frequency bands

Contrast	Regions	BA	*k*	Cluster $p_{FDR\text{-}corr.}$	MNI coordinates x	y	z	Peak *t* value	Peak Z-value
	LF (0.01-0.027 Hz)								
HC>HIV	L IPL	40	160	0.022	−52	−36	42	5.04	4.96
	L IFG, **dlPFC, mPFC, premotor**	44, 45, 46, 9, 6	770	0.000	−40	4	38	4.92	4.84
	R IFG, premotor	44, 6	278	0.003	46	10	36	4.85	4.78
	L IFG	44	179	0.019	−44	24	18	4.74	4.67
HC>PD	L **dlPFC, mPFC**	9, 46	685	0.000	−20	24	46	5.56	5.45
	L **premotor**	6	158	0.037	−38	2	26	5.32	5.22
	L **dlPFC**	9, 46	217	0.014	−28	42	32	4.81	4.74
	L Putamen/Pallidum		123	0.060	−18	4	6	3.93	3.89
HIV>HC	R ITG	37	250	0.005	58	−60	−16	5.83	5.70
	R Lingual	18	272	0.005	14	−64	2	4.82	4.75
	L SMA, paracentral	6	116	0.036	−8	−4	74	4.69	4.62
	R Precentral, premotor	4, 6	145	0.029	58	−4	42	4.50	4.44
	L OFG, rectus	11	181	0.016	−2	42	−20	4.47	4.41
	R Post-/Precentral	3,4	117	0.036	28	−30	66	4.44	4.38
	L STG, Rol. Oper.	42	120	0.036	−56	−6	10	4.10	4.05
HIV>PD	R Pre-/Postcentral	6, 4, 43, 3	1767	0.000	44	−28	24	5.63	5.51
	L STG/Rol. Oper.	42	652	0.000	−50	−8	16	5.52	5.41
	R Lingual	18	118	0.036	14	−70	2	4.77	4.70
	L Pre-/Postcentral	6, 4, 3	200	0.010	−46	−12	50	4.58	4.52
	L SMA, paracentral	6	134	0.032	−2	−8	72	4.56	4.50
	R insula, putamen	13	128	0.032	34	−4	10	4.26	4.21
	B OFG, rectus	11	146	0.030	0	40	−18	4.05	4.01
	R Hippocampus[b]		35	0.005[a]	34	−8	−16	4.15	4.10
PD>HC	R MOG	17	196	0.014	26	−96	8	5.39	5.29
	B OFG, rectus	11	158	0.027	−4	58	−22	5.01	4.92
	L MOG	1	214	0.014	−28	−82	26	4.00	3.95
PD>HIV	L SOG	19	181	0.034	−26	−78	30	4.24	4.19
	L MOG	18	189	0.034	−20	−96	20	4.10	4.06
	M1 (0.027-0.073 Hz)								
HIV>HC	R ITG	37	250	0.007	58	−60	−16	5.12	5.03
HIV>PD	R Hippocampus[b]		53	0.003[a]	34	−8	−16	4.28	4.23
	L Hippocampus[b]		30	0.008[a]	−30	−8	−16	4.02	3.98

Contrast	Regions	BA	*k*	Cluster $p_{FDR\text{-}corr.}$	MNI coordinates x	y	z	Peak *t* value	Peak Z-value
PD>HC	L MOG	17, 18	516	0.000	−26	−92	14	4.43	4.37
	R MOG	17, 18	187	0.026	26	−98	8	4.30	4.24
PD>HIV	L MOG	17, 18	242	0.014	−20	−98	12	4.49	4.43
	M2 (0.073-0.17 Hz)								
HIV>PD	B Cerebellum		178	0.021	6	−42	−42	5.10	5.01
	R Hippocampus		140	0.028	32	−6	−16	4.69	4.62
	L Hippocampus[b]		24	0.015[a]	−26	−8	−18	3.85	3.81
	HF (0.17-0.25 Hz)								
HC>PD	B Cerebellum		247	0.006	6	−42	−42	5.12	5.03
HIV>PD	B Cerebellum		311	0.002	6	−42	−42	5.72	5.60
	L Pallidum[b]		26	0.008[a]	−14	2	0	3.71	3.68

Whole brain SPM maps, cluster threshold $p_{corrected}<0.05$.

[a] peak threshold $p_{FWE\ corrected}<0.05$,

[b] small volume correction.

Abbreviations: Study groups by diagnosis: Healthy control (HC) group, HIV infection (HIV) group, Parkinson's disease (PD) group; R: right; L: left; B: bilateral; BA: Brodmann area; k: number of brain voxels in a cluster; MNI coordinates (x,y,z) for peak voxels within a significant cluster; IPL: inferior parietal lobe; IFG: inferior frontal gyrus, dlPFC: dorsolateral prefrontal cortex; mPFC: medial prefrontal cortex; OFG: orbitofrontal gyrus; SMA: supplementary motor area; Rol. Oper.: Rolandic operculum; ITG: inferior temporal gyrus; STG: superior temporal gyrus; SOG: superior occipital gyrus; MOG: middle occipital gyrus.

Table 3A.

ALFF and motor performance in the HIV group

A. HIV							
Regions	***F-band***	***stand.beta***	***p***			***stand.beta***	***p***
Parkinsonian symptoms	R^2=.38, F(4,25)=3.79, p=0.015			*correlation* [a]		*age contribution*	
(UPDRS-III)	**R^2 change=.31**, F(2,25)=6.28, p=0.006			*r*	*p*		
Amygdala	M1	.978	0.048	.48	0.008	.051	ns
Thalamus	M1	2.552	0.018	−.41	0.023		
Ataxia	R^2=.58, F(6,23)=5.35, p=0.001			*correlation* [a]		*age contribution*	
(SARA)	**R^2 change=.43**, F(4,23)=5.86, p=0.002			*r*	*p*		
Amygdala	M1	.331	0.035	.38	0.041	.030	ns
Thalamus	LF	−.336	0.026	−.48	0.009		
L. precentral, premotor	LF	−.277	ns	−.45	0.015		
B. cerebellum	HF	.154	ns	.42	0.022		

Hierarchical multiple regression analyses tested the contribution (R^2 change) of regional ALFF (step 2) while controlling for age and rs-fMRI motion (step 1).

[a]Partial correlation controlling for age and rs-fMRI motion

Table 3B.

ALFF and motor performance in the PD group

Regions	**F-band**	**stand.beta**	**p**			**stand.beta**	**p**
Parkinson symptoms	R^2=.34, F(5,29)=2.94, p=0.029			*correlation* [a]		*age contribution*	
(UPDRS-III *on meds*)	**R^2 change=.34**, F(3,29)=4.90, p=0.007			*r*	*p*		
L. SMA, paracentral	LF	.347	0.031	.39	0.027	.060	ns
R. precentral, premotor	LF	.283	0.087	.37	0.034		
R. MOG	LF	−.299	0.076	−.35	0.043		
	R^2=54, F(5,29)=6.93, p<0.0001			*correlation* [a]		*age contribution*	
(UPDRS-III *off meds*)	**R^2 change=.47**, F(3,29)=10.03, p<0.0001			*r*	*p*		
Caudate	HF	.305	0.026	.36	0.037	−.230	0.093
R. precentral, premotor	LF	.436	0.003	.49	0.004		
L. MOG	LF	.333	0.026	.41	0.018		
Ataxia	R^2=50, F(5,29)=5.68, p=0.001			*correlation* [a]		*age contribution*	
(SARA *on meds*)	**R^2 change=.43**, F(3,29)=9.21, p<0.0001			*r*	*p*		
L. putamen	LF	−.269	0.058	−.35	0.048	−.075	ns
L. dlPFC, dACC	LF	.452	0.006	.37	0.033		
L. SMA, paracentral	LF	.526	0.001	.46	0.007		
	R^2=65, F(8,25)=5.74, p<0.0001			*correlation* [a]		*age contribution*	
(SARA *off meds*)	**R^2 change=.60**, F(6,25)=7.13, p<0.0001			*r*	*p*		
Putamen	LF	−.392	0.014	−.48	0.006	−.180	ns
Thalamus	M2	−.423	0.005	−.41	0.020		
R. hippocampus	M1	.417	0.019	.35	0.049		
L. hippocampus	M1	.049	ns	.35	0.051		
L. MOG	LF	.241	ns	.38	0.031		
L. dlPFC, dACC	LF	.114	ns	.41	0.019		

Hierarchical multiple regression analyses tested the contribution (R^2 change) of regional ALFF (step 2) while controlling for age and rs-fMRI motion (step 1).

[a]Partial correlation controlling for age and rs-fMRI motion

Table 4A.

ALFF and cognitive performance in the HIV group

Regions	**F-band**	**stand.beta**	**p**			**stand.beta**	**p**
Global cognition	R^2=55, F(9,20)=2.74, p=0.029			*correlation* [a]		*age contribution*	
(DRS-2)	**R^2 change=.53**, F(7,20)=3.36, p=0.016			*r*	*p*		
Caudate	M2	−.173	ns	−.35	.067	−.200	ns
Putamen	HF	−.041	ns	−.45	.016		
Hippocampus	LF	−.243	ns	−.47	.012		
L. OFG, rectus	LF	−.274	ns	−.42	.026		
L. IPL	LF	.334	0.080	.39	.042		
L. MOG	LF	−.112	ns	.47	.011		
L. SOG	LF	.4l8	ns	.52	.004		
IP speed	R^2=.79, F(11,18)=6.08, p<0.0001			*correlation* [a]		*age contribution*	
(SDMT)	**R^2 change=.62**, F(9,18)=5.81, p=0.001			*r*	*p*		
Amygdala	HF	−.631	.063	−.48	0.008	−.410	0.014
Amygdala	M2	.641	ns	−.48	0.009		
Amygdala	M1	−.273	ns	−.47	0.010		
Amygdala	LF	.327	ns	−.37	0.047		
Hippocampus	LF	−.411	0.046	−.39	0.037		
L. SMA, paracentral	LF	−.167	ns	−.44	0.017		
L. MOG	LF	.180	ns	.39	0.038		
R. MOG	LF	.204	ns	.46	0.012		
R. ITG	LF	.627	0.0001	.40	0.034		
Executive function	R^2=.52, F(6,22)=4.02, p=0.007			*correlation* [a]		*age contribution*	
(Stroop color-word)	**R^2 change=.32**, F(4,22)=3.66, p=0.020			*r*	*p*		
Putamen	M1	.350	0.045	.49	0.010	−.627	0.001
Thalamus	LF	.133	ns	.44	0.021		
R. ITG	LF	.108	ns	.42	0.028		
R. ITG	M1	.256	ns	.43	0.024		
Attention	R^2=.35, F(4,25)=3.31, p=0.026			*correlation* [a]		*age contribution*	
(Digit span forward)	**R^2 change=.29**, F(2,25)=5.53, p=0.010			*r*	*p*		
Hippocampus	LF	−.433	0.043	−.49	0.007	−.178	ns
L. IPL	LF	.334	.068	.43	0.024		
Immediate memory	R^2=17, F(3,26)=1.78, p=0.176			*correlation* [a]		*age contribution*	
(CVLT-IM)	**R^2 change=.16**, F(1,26)=5.04, p=0.033			*r*	*p*		
L. IPL	LF	.419	0.033	.40	0.033	−.166	ns

Regions	**F-band**	**stand.beta**	**p**			**stand.beta**	**p**
Long-delay memory	R^2=41, F(6,23)=2.69, p=0.040			*correlation* [a]		*age contribution*	
(CVLT-LD)	**R^2 change=.41**, F(4,23)=4.02, p=0.013			*r*	*p*		
Hippocampus	LF	−.318	ns	−.39	0.035	.041	ns
Pallidum	M1	.411	0.049	.37	0.048		
B. OFG, rectus	LF	−.025	ns	−.41	0.026		
L. MOG	LF	.348	0.097	.42	0.024		

Hierarchical multiple regression analyses tested the contribution (R^2 change) of regional ALFF (step 2) while controlling for age and rs-fMRI motion (step 1).

[a]Partial correlation controlling for age and rs-fMRI motion

Table 4B.

ALFF and cognitive performance in the PD group

Regions	**F-band**	**stand.beta**	**p**			**stand.beta**	**p**
Global cognition	R^2=.35, F(4,30)=4.10, p=0.009			*correlation* [a]		*age contribution*	
(DRS-2)	**R^2 change=.30**, F(2,30)=6.99, p=0.003			*r*	*p*		
Amygdala	LF	−.562	0.001	−.56	0.001	−.173	ns
R. hippocampus	LF	.021	ns	−.36	0.037		
IP speed	R^2=.54, F(4,31)=9.16, p<0.0001			*correlation* [a]		*age contribution*	
(SDMT)	**R^2 change=.27**, F(2,31)=9.05, p=0.001			*r*	*p*		
Amygdala	LF	−.395	0.003	−.46	0.007	−.423	0.002
B. OFG, rectus	LF	.353	0.008	.40	0.019		
Executive function	R^2=.46, F(3,32)=9.17, p<0.0001			*correlation* [a]		*age contribution*	
(Stroop color-word)	**R^2 change=.09**, F(1,32)=5.17, p=0.030			*r*	*p*		
Amygdala	M1	−.296	0.030	−.37	0.030	−.507	0.001
	R^2=.54, F(4,31)=3.14, p=0.028			*correlation* [a]		*age contribution*	
(Digit span backward)	**R^2 change=.22**, F(2,31)=4.80, p=0.015			*r*	*p*		
Hippocampus	M2	−.338	0.060	−.36	0.036	.109	ns
L. IPL	LF	−.319	0.046	−.38	0.028		
Attention	R^2=.16, F(3,32)=2.03, p=0.013			*correlation* [a]		*age contribution*	
(Digit span forward)	**R^2change=.15**, F(1,32)=5.77, p=0.022			*r*	*p*		
L. IPL	LF	−.390	0.022	−.39	0.022	.107	ns
Immediate memory	R^2=.24, F(4,31)=2.44, p=0.068			*correlation* [a]		*age contribution*	
(CVLT-IM)	**R^2 change=.21**, F(2,31)=4.30, p=0.023			*r*	*p*		
Amygdala	M1	−.424	ns	−.47	0.006	−.099	ns
Amygdala	M2	−.046	ns	−.39	0.024		
Long-delay memory	R^2=.44, F(6,29)=3.80, p=0.007			*correlation* [a]		*age contribution*	
(CVLT-LD)	**R^2 change=.41**, F(4,29)=5.26, p=0.003			*r*	*p*		
Caudate	HF	−.334	0.025	−.34	0.048	−.141	ns
L. Putamen	LF	.307	0.066	.44	0.009		
R. Lingual	LF	−.272	0.079	−.41	0.016		
L. MOG	LF	−.152	ns	−.38	0.025		
Visuospatial function	R^2=.36, F(6,29)=2.73, p=0.032			*correlation* [a]		*age contribution*	

Regions	**F-band**	**stand.beta**	**p**			**stand.beta**	**p**
(JLO)	***R*² change=.32**, $F(4,29)=3.66$, $p=0.016$			r	p		
Hippocampus	M2	−.199	ns			−.116	ns
Caudate	M2	.130	ns				
Putamen	LF	.258	ns				
L. mid. insula, putamen	LF	.277	ns				

Hierarchical multiple regression analyses tested the contribution (R^2 change) of regional ALFF (step 2) while controlling for age and rs-fMRI motion (step 1).

[a]Partial correlation controlling for age and rs-fMRI motion